J. Phys. B: At. Mol. Opt. Phys. **29** (1996) 1531–1547. Printed in the UK

Low-energy electron impact excitation of the nitrogen molecule: optically forbidden transitions

Charles J Gillan†, Jonathan Tennyson‡, Brendan M McLaughlin§ and Philip G Burke†

† Department of Applied Mathematics and Theoretical Physics, The Queen's University of Belfast, Belfast BT7 1NN, UK

‡ Department of Physics and Astronomy, University College London, London WC1E 6BT, UK

§ Institute for Theoretical Atomic and Molecular Physics, Harvard-Smithsonian Center for Astrophysics, 60 Garden Street, Cambridge, MA 02138, USA

Received 18 December 1995

Abstract. *Ab initio* calculations are performed on the e^-–N_2 scattering system, at low impact energies, using the *R*-matrix technique. The X $^1\Sigma_g^+$ ground state and the lowest seven valence excited states, A $^3\Sigma_u^+$, B $^3\Pi_g$, W $^3\Delta_u$, B′ $^3\Sigma_u^-$, a′ $^1\Sigma_u^-$, a $^1\Pi_g$ and w $^1\Delta_u$, of N_2 are included in the close coupling expansion with each state being represented by a configuration interaction wavefunction in a hybrid orbital set. Various approximations for the representation of the correlation between the target and the incident electron are investigated. Integrated and differential scattering cross sections are presented, and compared to experiment, for excitation from the ground level to optically forbidden levels. The results compare favourably with recent experiments in this energy region and remove a number of problems with our previous work.

1. Introduction

To comprehend the properties of many astrophysical objects it is important to understand the process by which electrons lose energy in a gas containing molecular nitrogen (N_2), carbon monoxide (CO) or carbon dioxide (CO_2). Cross sections for e^-–N_2, e^-–CO and e^-–CO_2 excitation are of importance for estimating electron energy deposition in the atmospheres of Earth, Mars and Venus (Fox and Dalgarno 1979, Fox and Victor 1988, Liu and Victor 1994). They are also of importance in understanding the aurora air glow, the Titan day glow (Ajello and Shemansky 1985, Fox 1993) and in the resolution of the aurora 2150 Å UV mystery (Dalgarno *et al* 1981, Dalgarno and Victor 1982). N_2 is an efficient electron absorber due to the presence of a large shape resonance in the $^2\Pi_g$ scattering symmetry near 2 eV. For atmospheric research one source of hot, excited nitrogen atoms is via predissociation after collisional excitation of N_2 (Schematovich *et al* 1992). The atmosphere of Triton is similar to that of Titan with its major constituent being molecular nitrogen as indicated by Dalgarno and Fox (1994). N_2 may be found in the interstellar medium (ISM), although being a homonuclear species, without ro-vibrational emissions in the ground state, it is very hard to detect. However, once formed, it lives a very long time due to its large dissociation and ionization energy. Electron and photon collisions with nitrogen molecules are therefore of fundamental interest in understanding ionospheric and auroral phenomena in the Earth's upper atmosphere and in many gaseous discharge processes (Itikawa *et al* 1986). The work

0953-4075/96/081531+17$19.50

presented here is restricted to electronic excitation cross sections by electron impact of molecular nitrogen.

The nitrogen molecule, N_2, is a triply bonded system with a very stable electronic ground state. As a result bound state calculations on excited electronic states of N_2 present a major challenge to computational chemistry and this has been exemplified in the work of Ermler *et al* (1981); figure 1 shows the potential energy curves for the lowest 13 states of N_2 as computed by these authors using a configuration space which involved single and double electron excitations (SD) from the N_2 valence space. Typically the theoretical treatment of low-energy light particle impact phenomena employs the close coupling expansion which involves an expansion over unperturbed target eigenstates; it is the quality of representation of those target states which can ultimately place a constraint on the accuracy of any scattering model. An additional constraint lies in the fact that the scattering wavefunction must take a balanced account of the correlation between the target and the scattering particle. The Schrödinger equation for electron scattering by the N_2 molecule produces a partial differential equation in 45 spatial variables; the power of the close coupling expansion is that it removes the dependence on 42 of those variables replacing them by a sum over target eigenstates. Unfortunately, this is an infinite sum. The target states are hard to represent properly and it is also difficult to retain a large number of them in the scattering model; as a result there have only been, as far as we are aware, a few previous computational studies with modern *ab initio* program suites, of low-energy electron impact excitation of N_2 (Gillan *et al* 1990, Huo *et al* 1987, Huo 1990). These calculations, while being *state of the art* at the time of publication, were limited in their representation of the N_2 bound states with Huo *et al* (1987) and Huo (1990) using one configuration per state and Gillan *et al* (1990) using a very small configuration interaction approximation. Recently Schneider and Gianturco (1996) have studied resonances in N_2^- using a large scale CI method.

On the experimental side the major work on this system has been carried out by Cartwright *et al* (1977a, b), Trajmar *et al* (1983), Zetner and Trajmar (1987) and Brunger and Teubner (1990) with all of these authors considering several of the transitions in the valence manifold of N_2. The particular transition $X\ ^1\Sigma_g^+ \rightarrow a\ ^1\Pi_g$ has received the attention of Ajello and Shemansky (1985) and Mason and Newell (1987). Additional experimental work (Zipf and McLaughlin 1978, Zipf and Gorman 1980, Filippelli *et al* 1984) has concentrated on using electron impact excitation to obtain optical data on the $c_4'\ ^1\Sigma_u^+ \rightarrow X\ ^1\Sigma_g^+$, $b\ ^1\Pi_u \rightarrow X\ ^1\Sigma_g^+$, $b'\ ^1\Sigma_u^+ \rightarrow X\ ^1\Sigma_g^+$ and $D\ ^3\Sigma_u^+ \rightarrow B\ ^3\Pi_g$ electronic transitions.

For technical reasons, associated with the apparatus, the only measurements frequently made for electron scattering by molecules are angular distributions. Often these are only possible over a restricted range of scattering angle. Thus, unless numerical extrapolation techniques are used with their inherent potential for error, it is not usually possible for this kind of experiment to yield total cross sections. This means that theorists must compute differential cross sections in order to compare with experiment; these observables tend to be a much more sensitive test of the convergence of various expansions used in the model. Augmenting the confusion is the fact that there are some discrepancies between the angular distribution measurements of different groups. It is in this situation that a better computational model can shed some light on the problem.

The fact that this molecule is of fundamental importance in the atmosphere of our planet, not least in the study of flow fields surrounding high-velocity space vehicles at re-entry, encouraged us to enhance our previous work which was published several years ago as the first application of the UK *R*-matrix codes to electron impact excitation of the nitrogen molecule (Gillan *et al* 1990). Since that time we have gained, by considering targets with

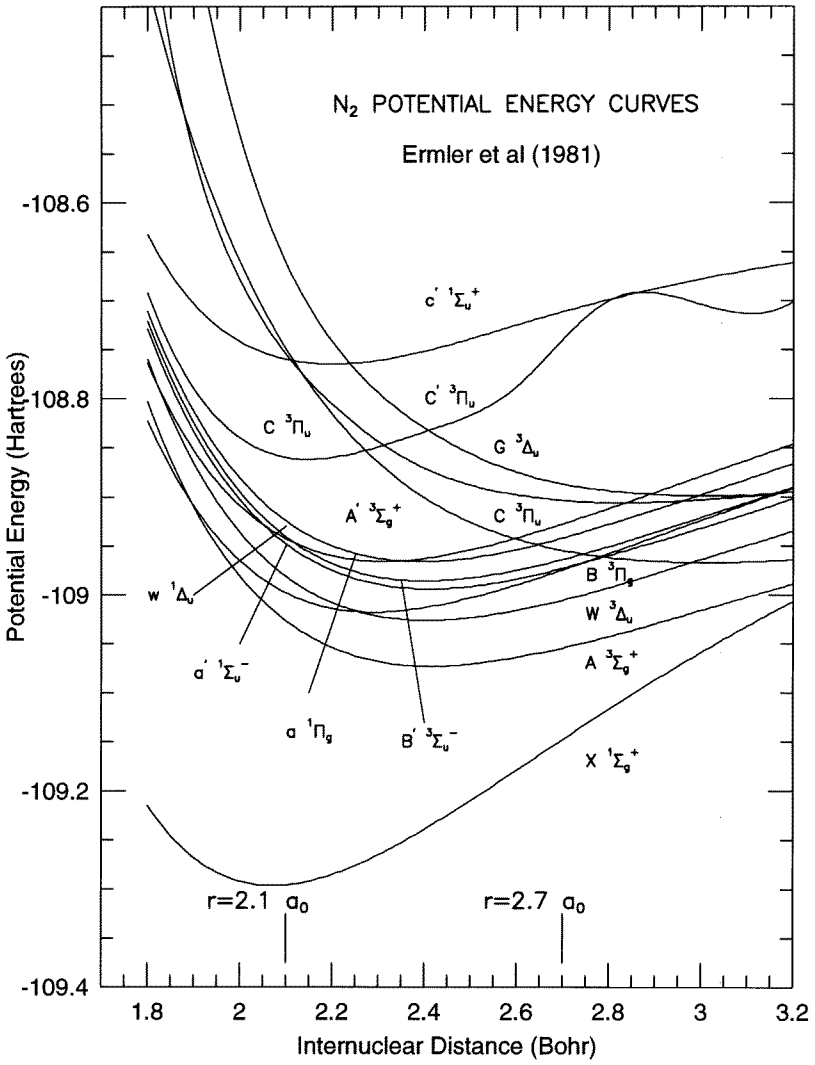

Figure 1. Potential energy curves computed by Ermler *et al* (1981) for the lowest 13 valence states of N_2. This figure has been generated by plotting the results given by these authors for the SD model in table VI of their paper.

fewer electrons (Branchett *et al* 1990, McLaughlin *et al* 1993, McLaughlin and Gillan 1995), considerable experience in modelling electron impact excitation of diatomic molecules. At the same time we have eliminated some deficiencies in our computer program suite which we now believe had an adverse effect on our previous e^-–N_2 results. This paper therefore reports on a more comprehensive, and we believe more accurate, calculation on electron scattering from the N_2 system. When a single configuration closed shell target state is used in a scattering model, as is frequently the case in studies of elastic scattering in e^-–N_2, the correlation of the incident electron with the motions of the target electrons is introduced into the model using two particle–one hole terms (Gillan *et al* 1987). The situation is not so straightforward when configuration interaction targets are used so we have studied the various ways in which we can represent this correlation in our *R*-matrix studies.

In the next section, the computational method is discussed, while the subsequent section presents details of the scattering calculations. Our results for total and differential cross sections for several transitions are shown in section 4 where they are compared with experiment. In section 5, we discuss our results, and in particular the models used, and conclude, in section 6, by indicating future directions for this research.

2. Computational method

Our numerical experiments have been performed using the *R*-matrix method in the form developed by the UK group; algorithmic, computational and numerical features of the computer program suite have been described by Gillan *et al* (1995). The *R*-matrix method is an *ab initio* approach to the solution of the scattering problem on an equal level with the complex Kohn and Schwinger multi-channel methods (Rescigno *et al* 1995, Huo 1995) and has in fact benefited substantially from parallel developments in these software packages. Our implementation of the technique has been described in detail in several other publications, so only a brief summary is given here for the sake of completeness. McLaughlin *et al* (1993) have discussed the application of the method, in great detail, for a two-state excitation calculation on e^-–He_2^+ scattering while Morgan and Tennyson (1993) and Higgins *et al* (1994) have reported on *R*-matrix studies of electronic excitation in e^-–CO and e^-–O_2 scattering, respectively, with the latter work having been recently extended to include vibrational motion (Higgins *et al* 1995). The reader should realize, however, that, while a tried and tested computational procedure is employed here, there is a considerable difference in the chemistry of the molecules CO, O_2 and N_2 and therefore in the physics of the electron scattering process.

We have invoked the fixed nuclei approximation meaning that the work reported here has been carried out with the nuclei fixed at an internuclear separation of 2.1 a_0. Our previous work (Gillan *et al* 1990) was carried out at the equilibrium internuclear separation (2.068 a_0) of the ground state of N_2. Unfortunately, the lowest valence states are very sensitive to small changes in the target-state representation at that geometry, their equilibria lying to the right of the ground-state minimum. Choosing an internuclear separation that is slightly closer to the valence-state minima reduced the aforementioned sensitivity as well as giving a slightly larger energy separation between the valence-state thresholds.

Configuration space is divided into two parts known as the inner and outer regions, with the former being a hypersphere defined by $r_i < 10.0\ a_0\ \forall i$, where r_i is the radial distance of electron i from the centre of mass of the two nitrogen nuclei. The outer region, in the electron scattering problem, is defined by $r_i < 10.0\ a_0$ for $i = 1, N$ and $r_{N+1} > 10.0\ a_0$ for an N electron target. The *R*-matrix radius of 10.0 a_0 is large enough that the target state charge distributions are completely enveloped by the hypersphere. We checked the stability of our calculations with respect to variations of this choice but found that 10.0 a_0 was quite adequate, due, no doubt, to the fact that we are dealing only with valence states of the target.

The solution to the non-relativistic Schrödinger equation for the scattering problem is given by Ψ_E,

$$\Psi_E = \sum_k A_{Ek}\psi_k \tag{1}$$

where the ψ_k are energy-independent basis functions and the A_{Ek} are coefficients whose value changes as we change the total energy E. The power of *R*-matrix theory lies in the fact that these ψ_k are independent of energy and need be constructed only once for all

scattering energies. The form of the ψ_k is

$$\psi_k(\boldsymbol{x}_1, \ldots, \boldsymbol{x}_{N+1}) = \mathcal{A} \sum_{ij} \bar{\Phi}_i(\boldsymbol{x}_1, \ldots, \boldsymbol{x}_N, \sigma_{N+1}) \eta_j(\boldsymbol{r}_{N+1}) \alpha_{ijk} + \sum_j \chi_j(\boldsymbol{x}_1, \ldots, \boldsymbol{x}_{N+1}) \beta_{jk} \tag{2}$$

where $\mathcal{A}$ is the anti-symmetrization operator and $\boldsymbol{x}_i = (\boldsymbol{r}_i, \sigma_i)$ stands for the space and spin coordinates of the ith electron. The functions $\bar{\Phi}_i$ are eigenfunctions of the total spin operator, S^2, and its z-component, S_z, formed by coupling the products of the spin function of the continuum electron with the target electronic states Φ_i. The η_j functions are continuum molecular orbitals which are non-zero on the boundary of the inner region. The second summation is over square integrable (L^2) functions, χ_j, descriptive of states with all of the electrons in bound orbitals. At the very least the χ_j must include the orthogonality terms as defined by Gillan *et al* (1995); they are sometimes referred to as penetration terms (Rescigno *et al* 1995).

3. Scattering calculations

Two principal features distinguish one R-matrix scattering calculation from another, given a specific target and a particular choice for the bound and continuum basis functions. These are the configuration spin function (CSF) expansions used for the target wavefunctions and the CSF expansion used in constructing the scattering wavefunction. This is because the R-matrix method is based on the configuration interaction representation of the wavefunction in a common set of orthogonal orbitals. Thus we now consider each of these aspects in turn.

3.1. Target state representation

The R-matrix method, in common with most other *ab initio* methods based upon a configuration interaction representation of the collision process, depends internally on a configuration interaction representation of those target states retained in the close coupling expansion. Due to practical considerations associated with the size of the scattering Hamiltonian, one is required to keep the target-states representation as compact as possible but nevertheless to use target eigenfunctions which have not only *relative* energies but also *absolute* moments and transition moments which are as accurate as possible. The constraint, mentioned earlier, that a single set of orthogonal molecular orbitals must be used, is imposed solely by the algorithms used in our program suite.

A detailed study of the valence states of the nitrogen molecule has been presented by Ermler *et al* (1981). For the reasons outlined below it was not possible for us to use the work of Ermler *et al* (1981) directly, although we have used their basis of Slater-type functions (STFs). Initially we computed a Hartree–Fock–Roothaan self-consistent field (SCF) wavefunction for the X $^1\Sigma_g^+$ ground state of N_2 and used the resulting orbitals to initiate a complete active space self-consistent field calculation (CASSCF) on the ground state and on each of the seven valence excited states A $^3\Sigma_u^+$, B $^3\Pi_g$, W $^3\Delta_u$, B′ $^3\Sigma_u^-$, a′ $^1\Sigma_u^-$, a $^1\Pi_g$ and w $^1\Delta_u$; the active space was the valence space, as discussed by Ermler and McLean (1980), and consists of the orbitals

$$1\sigma_g\, 1\sigma_u\, 2\sigma_g\, 2\sigma_u\, 3\sigma_g\, 1\pi_u\, 1\pi_g\, 3\sigma_u.$$

The result of each CASSCF evaluation was a set of molecular orbitals which are optimum for the particular state in question. A common orthogonal orbital set was constructed by

picking various hybrid orbital sets from our CASSCF results, an approach similar to that employed by Tennyson (1988). The hybrid orbital set giving the best overall target state model is described in table 1. In the scattering calculations, the target states were generated by using the same valence CI approximation but in the fixed hybrid orbital set; the computed eigenenergies are presented in table 2 where they are compared with the work of Ermler *et al* (1981). For the states considered, our excitation energies agree with those of Ermler *et al* at the 4–8% level.

Table 1. Source of the orbitals used in building the hybrid orbital set used in expanding the target states of N_2 and in generating the L^2 basis for the scattering calculations described in the text.

Orbital designation	Origin
$1\sigma_g$, $2\sigma_g$, $3\sigma_g$, $1\sigma_u$, $2\sigma_u$, $3\sigma_u$	X $^1\Sigma_g^+$ state (CASSCF)
$1\pi_u$, $1\pi_g$	W $^3\Delta_u$ state (CASSCF)
$4\sigma_g$, $4\sigma_u$, $2\pi_u$, $2\pi_g$, $1\delta_g$, $1\delta_u$	X $^1\Sigma_g^+$ state (SCF)

Table 2. Absolute energies in Hartrees and relative energies in electron volts for the eight target states of N_2 expanded in the hybrid orbital set discussed in the text. These are compared with the singles and doubles (SD) results of Ermler *et al* (1981) which have been interpolated to the bond length of 2.1 a_0.

Target state designation	Number of CSFs	Absolute energy (Hartrees)	Excitation energy from X $^1\Sigma_g^+$ (eV)	Ermler *et al* (1981)
X $^1\Sigma_g^+$	96	−109.1215	0.00	0.00
A $^3\Sigma_u^+$	100	−108.8408	7.63	7.32
B $^3\Pi_g$	164	−108.8074	8.54	8.09
W $^3\Delta_u$	88	−108.7866	9.11	8.55
B′ $^3\Sigma_u^-$	68	−108.7602	9.83	9.46
a $^1\Pi_g$	120	−108.7577	9.89	9.61
a′ $^1\Sigma_u^-$	100	−108.7389	10.41	9.66
w $^1\Delta_u$	68	−108.7268	10.74	10.07

It is important to point out that this target description is substantially better than the one used in our previous paper (Gillan *et al* 1990) and although still limited, it gives a fairly consistent treatment of all eight target states discussed. In the recent work on O_2, which is doubly bonded, Higgins *et al* (1994), also used a valence CI approximation but employed only SCF orbitals; we have found, empirically, that a similar treatment is not adequate for N_2. Additionally, we have found that to improve on our present model we require an order of magnitude increase in the length of the CI expansions for each state!

3.2. Continuum problem: inner region

Our early work on elastic scattering in e^-–N_2 (Gillan *et al* 1987) used the two particle–one hole model to construct the $(N + 1)$ particle space, i.e. the CSF space for the scattering problem. This procedure is straightforward due to the fact that a single configuration closed shell target wavefunction was employed. Gillan *et al* (1995) have discussed the extension of this approximation to the situation in which a CI representation of the target states is used. In this paper we describe a further refinement of the approximation and compare

quantitatively the various levels involved using the $^2\Pi_g$ scattering symmetry as a specimen case.

Within each symmetry of the orbital set that we used in the scattering evaluation there were valence space orbitals defined in the previous section, single virtual orbital from the ground-state SCF calculation and a number of *continuum* orbitals; table 3 presents a summary of the total orbital set that we used. The virtual orbitals obtained in the SCF calculation are representative of a single electron outside a target charge cloud. In our scattering calculations we generate configurations in which the scattering electron populates these virtual orbitals. The virtual orbitals are two-centred with centres on each nitrogen nucleus. When these are expanded around the centre of mass of the system, where the continuum basis functions are located, they give rise to angular momentum values much higher than the few partial waves included in that numerical basis set.

Table 3. Division of the orbital set for each scattering symmetry.

Symmetry	Valence	Virtual	Continuum
Σ_g	$1\sigma_g$, $2\sigma_g$, $3\sigma_g$	$4\sigma_g$	$5, \ldots, 25\sigma_g$
Σ_u	$1\sigma_u$, $2\sigma_u$, $3\sigma_u$	$4\sigma_g$	$5, \ldots, 25\sigma_g$
Π_u	$1\pi_u$	$2\pi_u$	$3, \ldots, 23\pi_u$
Π_g	$1\pi_g$	$2\pi_g$	$3, \ldots, 15\pi_g$
Δ_g		$1\delta_g$	$2, \ldots, 14\delta_g$
Δ_u		$1\delta_u$	$2, \ldots, 14\delta_u$

Looking at the resonant $^2\Pi_g$ scattering symmetry in particular, the ψ_k can be analysed into parts as follows.

(1) The first part of each R-matrix basis function

$$1\sigma_g^2\, 1\sigma_u^2\, \{2\sigma_g 2\sigma_u 3\sigma_g 1\pi_u 1\pi_g 3\sigma_u\}^{10}\, (^1\Sigma_g^+)\{3\pi_g \ldots 15\pi_g\}^1\, (^2\Pi_g)$$

consists of the direct product of the Δ_i CSFs defining the target space with one electron in the continuum space.

(2) The L^2 part of each ψ_k may be further divided into three pieces:

(a) orthogonality (penetration) CSFs

$$1\sigma_g^2\, 1\sigma_u^2\, \{2\sigma_g 2\sigma_u 3\sigma_g 1\pi_u 1\pi_g 3\sigma_u\}^{10}\, (^1\Sigma_g^+)\{2\pi_g\}^1\, (^2\Pi_g)$$

accounting for the fact that the continuum molecular orbitals are also orthogonal to the unoccupied virtual orbitals;

(b) correlation CSFs

$$1\sigma_g^2\, 1\sigma_u^2\, \{2\sigma_g 2\sigma_u 3\sigma_g 1\pi_u 1\pi_g 3\sigma_u\}^{11} (^2\Pi_g).$$

where the scattering electron enters the charge cloud of the target state;

(c) two particle–one hole additional correlation CSFs

$$1\sigma_g^2\, 1\sigma_u^2\, \{2\sigma_g 2\sigma_u 3\sigma_g 1\pi_u 1\pi_g 3\sigma_u\}^9\, (Z) \otimes \{4\sigma_g, 4\sigma_u, 2\pi_u, 2\pi_g\}^2\, (^2\Pi_g).$$

These CSFs are analogous to the two particle–one hole terms for the SCF target but are vastly increased in number with a CI target. The quantity Z indicates that the nine remaining target electrons must have their coupling restricted to represent a target *hole*. For the N_2 ground state Z takes the values $^2\Sigma_g^+$, $^2\Sigma_u^+$, $^2\Pi_u$, $^2\Pi_g$ etc. The same analysis may be carried out for any scattering symmetry.

Note that the target eigenvector coefficients associated with each CSF have not yet been accounted for. They are in fact introduced to the type (1) configurations prior to

diagonalization of the Hamiltonian matrix. Our previous study (Gillan *et al* 1990) neglected phase differences which arise from treating N and $(N+1)$ electron CI problems. In the present work the correct phases were ensured by using a method presented by Orel *et al* (1991).

We have applied the above model, which we shall label case A, and have investigated two variations on it which we label cases B and C. In all models we must, of course, have the CSFs defined in (1) above, so that the difference between the models lies in the terms defined in (2). In cases B and C we omit CSFs of type 2(c). The CSFs of type (1) are contracted with the respective target-state eigenvectors in the final Hamiltonian. The CSFs of type 2(a) are similar in structure to type (1); in case C we have contracted these, also, with target-state eigenvectors.

3.3. Continuum problem: outer region

The outer region section of the collision problem was handled by adopting a single centre, no exchange, close coupling expansion of the wavefunction. R-matrix propagator (Baluja *et al* 1982) and accelerated Gailitis expansion methods (Noble and Nesbet 1984) were employed in the solution. The direct potential in these calculations contained contributions from ground- and excited-state quadrupole moments as well as all transition dipole moments coupling the eight target states. At each scattering energy the R-matrix was used to match outgoing wave solutions and their derivatives, a procedure which permits the evaluation of a K-matrix. Once the K-matrix is available, standard formulae may be invoked to produce physical observables for comparison with experiment.

4. Results

4.1. Comparison of models A, B and C

Although the aim of this work is to study electron impact electronic excitation, it is instructive to consider the behaviour of the well known $^2\Pi_g$ shape resonance. This resonance has been observed many times experimentally but direct comparisons with experiment are not possible without simultaneous treatment of nuclear motion. Instead, in table 5, we compare with the fixed geometry result of Morgan (1986) computed as part of a non-adiabatic nuclear motion calculation which gave good agreement with experiment. Of course this resonance has also been the subject of many theoretical studies, some of which are discussed below.

Figure 2(*a*) illustrates the partial cross section, symmetry $^2\Pi_g$, for the excitation $X\ ^1\Sigma_g^+ \rightarrow A\ ^3\Sigma_u^+$ computed with the three models A, B and C discussed in the previous section. The most striking feature of this figure is the very close agreement between the cross sections obtained using the three models.

Figure 2(*b*) compares the same results for the transition $X\ ^1\Sigma_g^+ \rightarrow B\ ^3\Pi_g$. In this case models A and B again give essentially the same results, although the cross sections obtained using model C have a much less pronounced peak at threshold than the other two models.

This indicates that the absence of the two particle–one hole terms (type 2(c) in section 3.2) does not here have an adverse effect on the modelling of the excitation process. Moreover, the extra contraction that has been introduced, case C, also has only a moderate effect. The problem of designing the best model will be discussed further below.

Table 4. Structure and dimension of the Hamiltonian for the $^2\Pi_g$ scattering symmetry.

Target states	CSFs	Continuum orbitals	Number	Total CSFs
$X\ ^1\Sigma_g^+$	96	π_g	13	1248
$A\ ^3\Sigma_u^+$	100	π_u	21	2100
$B\ ^3\Pi_g$	164	σ_g	21	3444
		δ_g	13	2132
$W\ ^3\Delta_u$	88	π_u	21	1848
$B'\ ^3\Sigma_u^-$	100	π_u	21	2100
$a'\ ^1\Sigma_u^-$	64	π_u	21	1344
$a\ ^1\Pi_g$	120	σ_g	21	2520
		δ_g	13	1560
$w\ ^1\Delta_u$	68	π_u	21	1428
			Subtotal	19 724
			L^2	1193
			Total CSFs	20 917

Table 5. Position and width of the $N_2^-\ ^2\Pi_g$ shape resonance for an internuclear separation of 2.1 a_0.

Calculation	E_r (eV)	Γ_r (eV)
Model A	2.785	0.719
Model B	2.916	0.728
Model C	3.024	0.770
Morgan (1986)	2.122	0.302

4.2. Integrated cross sections

Results for cross sections for the optically forbidden transitions from the $X\ ^1\Sigma_g^+$ state obtained using model B are shown in figure 3. They are compared with the energy-loss experimental measurements of Trajmar *et al* (1983) and in the case of the $X\ ^1\Sigma_g^+ \rightarrow A\ ^3\Sigma_u^+$ transition with the data from optical transmission measurements of Borst (1972). Note that the cusp in our $X\ ^1\Sigma_g^+ \rightarrow A\ ^3\Sigma_u^+$ cross sections at about 8.5 eV is associated with the $B\ ^3\Pi_g$ threshold.

On the whole there is good agreement between theory and experiment in the figures, in particular for the $X\ ^1\Sigma_g^+ \rightarrow B\ ^3\Pi_g$ transition, which is in marked contrast to our previous paper (Gillan *et al* 1990).

4.3. Differential cross sections

Differential cross sections were generated using the code of Malégat (1990), figures 4(a) and 4(b) show our differential cross sections, calculated using model B, for the excitation $X\ ^1\Sigma_g^+ \longrightarrow A\ ^3\Sigma_u^+$ at impact energies of 10 and 15 eV. At 15 eV, in figure 4(b), comparison is made with the measurements of Trajmar *et al* (1983) as well as the more recent data from Brunger and Teubner (1990). Since the latter authors did not report on any lower impact energy only the data from the former group is shown at 10 eV, figure 4(a). We have not shown the extrapolations to lower and higher angles that were computed by Trajmar *et al* (1983).

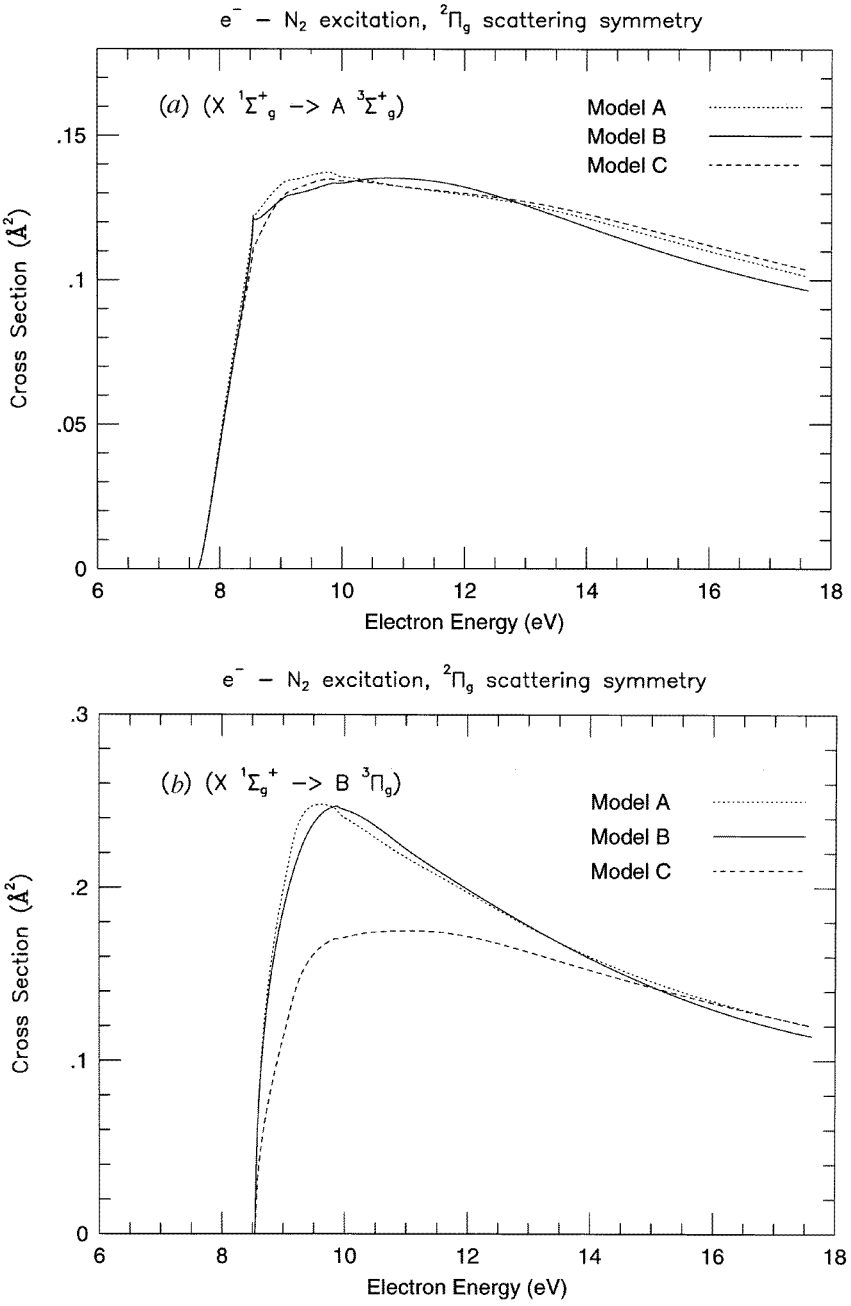

Figure 2. Comparison of integrated cross sections computed using configuration models A, B and C as explained in the text: (*a*) X $^1\Sigma_g^+ \rightarrow$ A $^3\Sigma_u^+$; (*b*) X $^1\Sigma_g^+ \rightarrow$ B $^3\Pi_g$.

Our calculations show that the excitation process is dominated by the $^2\Pi_g$ scattering symmetry, with a significant contribution from the $^2\Pi_u$ which is reflected in the overall shape of our differential cross sections. At both impact energies we obtain essentially the opposite behaviour to that exhibited by the Trajmar *et al* (1983) results, although at 15 eV

their large angle results are similar to ours. Also at 15 eV, our mid-range behaviour is in excellent agreement with the Brunger and Teubner results while at small angles we have a qualitatively similar shape to theirs. The fact that our calculation is within the fixed nuclei approximation, and therefore measures a slightly different physical process, may explain the difference between theory and experiment. Our theory however provides a consistent set of values for the differential cross sections across the entire angular range. This is a feature which is lacking in the experimental measurements.

5. Discussion

One objective of this study has been to analyse the different models used to construct scattering wavefunctions in the *R*-matrix method. The essential problem is one of balance. To obtain reliable calculations, especially for properties such as resonance position, it is essential to treat both the N electron target calculation and the $(N + 1)$ electron scattering calculations in an even-handed fashion. In particular it is important that the scattering calculation does not artificially improve the representation of the target. This is easily achieved for target single configuration (SCF) wavefunctions but is not nearly so straightforward when employing the multi-configuration (CI) expansions which are necessary for the accurate treatment of electronic excitation.

All three models employed here have been used in previous *R*-matrix calculations concerned with electron impact electronic excitation of molecules. This variety is caused by uncertainty over the best means of representing polarization in the scattering calculation. The coupled states expansions (configurations of type (1)) used in all coupled states calculations have a dual purpose. They provide the physical states into which electronic excitation occurs. They also provide flexibility in the target wavefunction which allows for polarization during the collision. For this reason most atomic *R*-matrix calculations use extra, 'pseudo' target states to represent the polarization interactions (Burke and Berrington 1993).

Including many target states in molecular calculations is computationally expensive and therefore models have been explored which allow for polarization effects by other means. The easiest way of doing this is via two particle–one hole (2p–1h) configurations (type (2c) above). Such configurations are the standard means of introducing polarization into calculations involving a single target state (Gillan *et al* 1987). For a single configuration target, Brillouin's theorem can be used to show that 2p–1h configurations cannot improve the representation of the target. Brillouin's theorem does not apply to CI wavefunctions and there is a real danger that in employing 2p–1h configurations one not only improves the representation of the target polarization but also the representation of the underlying target wavefunction.

Noble and Burke (1992) correctly predicted new resonances in the O_2^- system. However these workers, and subsequent calculations (Higgins *et al* 1994), have consistently found resonance positions which are too low in comparison with experiment. Noble and Burke included 2p–1h configurations in their model, which was similar to model A above. It is possible that these configurations artificially lowered their target states in the scattering calculations, thus giving the appearance of lowering the resonance positions.

Dropping 2p–1h configurations from the model, model B above, gives a model which is superficially free of the problems associated with model A. However, this is not strictly true. Within a complete active space (CAS) representation of the target wavefunctions such as the one used here, addition of an extra electron to the CAS, configurations type (2b) above, cannot alter the representation of the target. Conversely the use of unconstrained orthogonality (penetration) configurations, type (2a) above, can actually lead

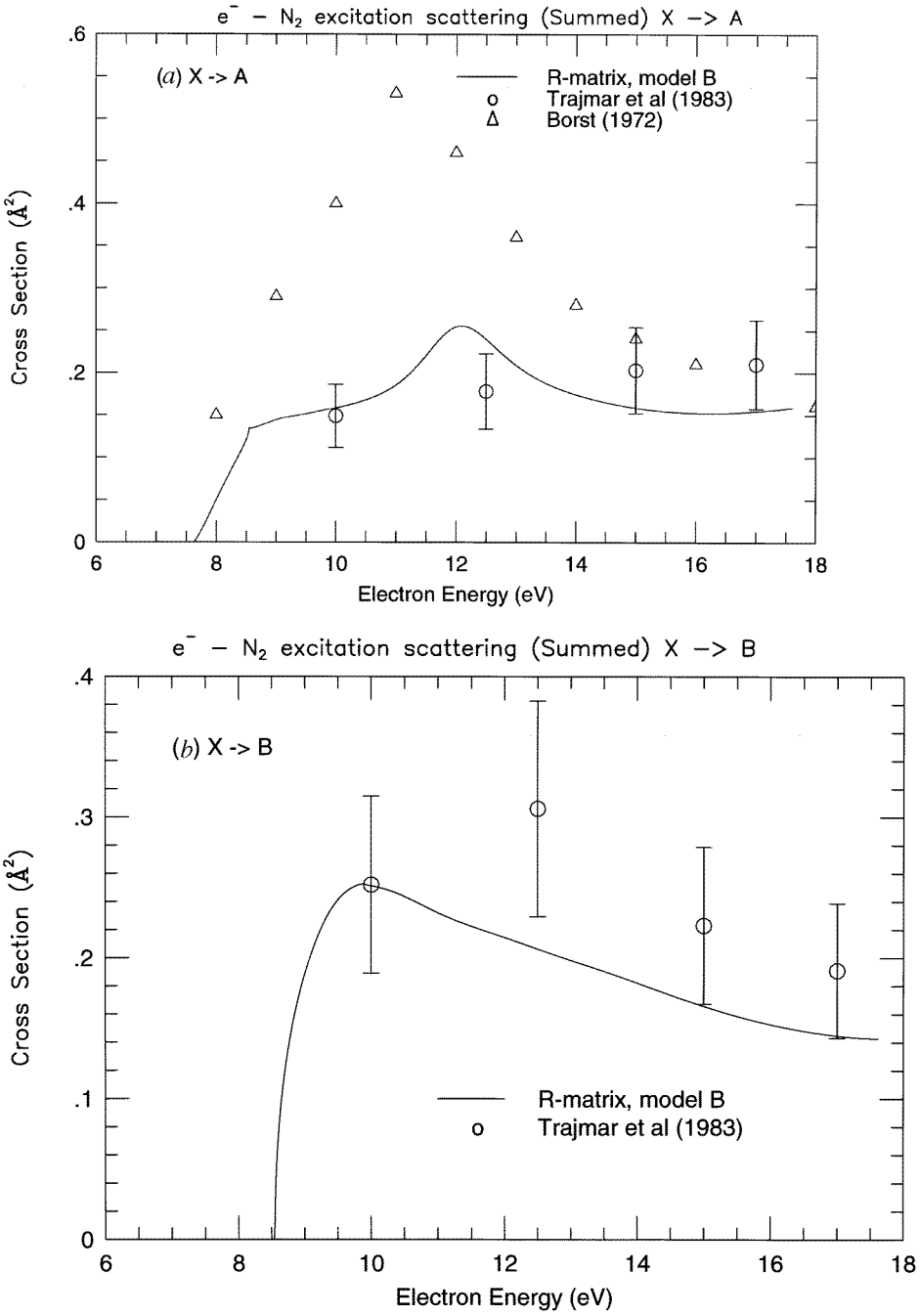

Figure 3. Total cross sections (Å^2) for the four transitions, (*a*) X $^1\Sigma_g^+ \rightarrow$ A $^3\Sigma_u^+$, (*b*) X $^1\Sigma_g^+ \rightarrow$ B $^3\Pi_g$, (*c*) X $^1\Sigma_g^+ \rightarrow$ W $^3\Delta_u$ and (*d*) X $^1\Sigma_g^+ \rightarrow$ B′ $^3\Sigma_u^-$. The full curves are our calculated data using model B and the experimental points are from Trajmar *et al* (1983), ○ , and from Borst (1972), △.

to improvements of the target wavefunction.

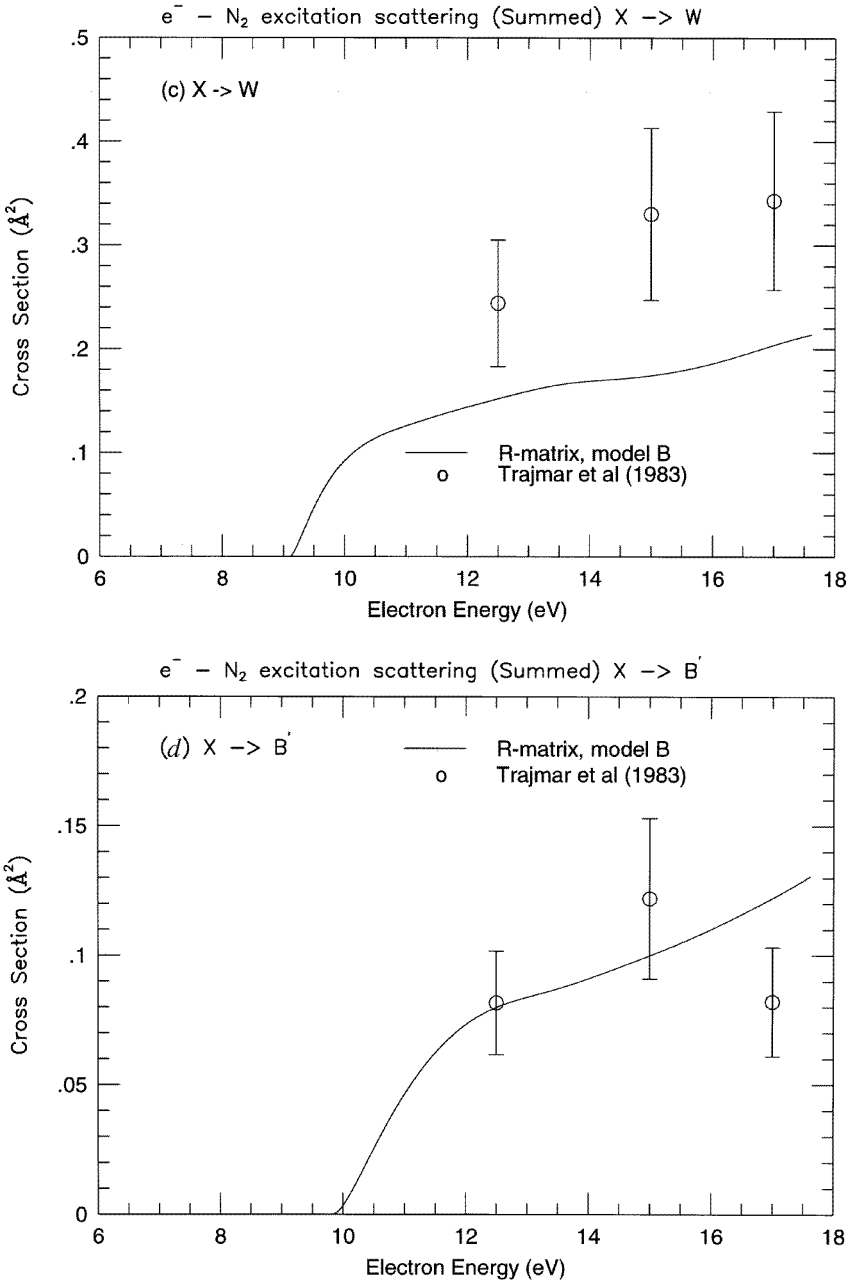

Figure 3. (Continued)

For this reason we have also explored model C, which contracts the orthogonality CSFs with the target wavefunction. This model is really 'pure' close coupling with no attempt to represent polarization effects by other means. Close coupling models have recently provided some excellent results when applied to atomic targets (Bray and Stelbovics 1995a, b). However, these calculations rely on very large close coupled expansions for simple (one

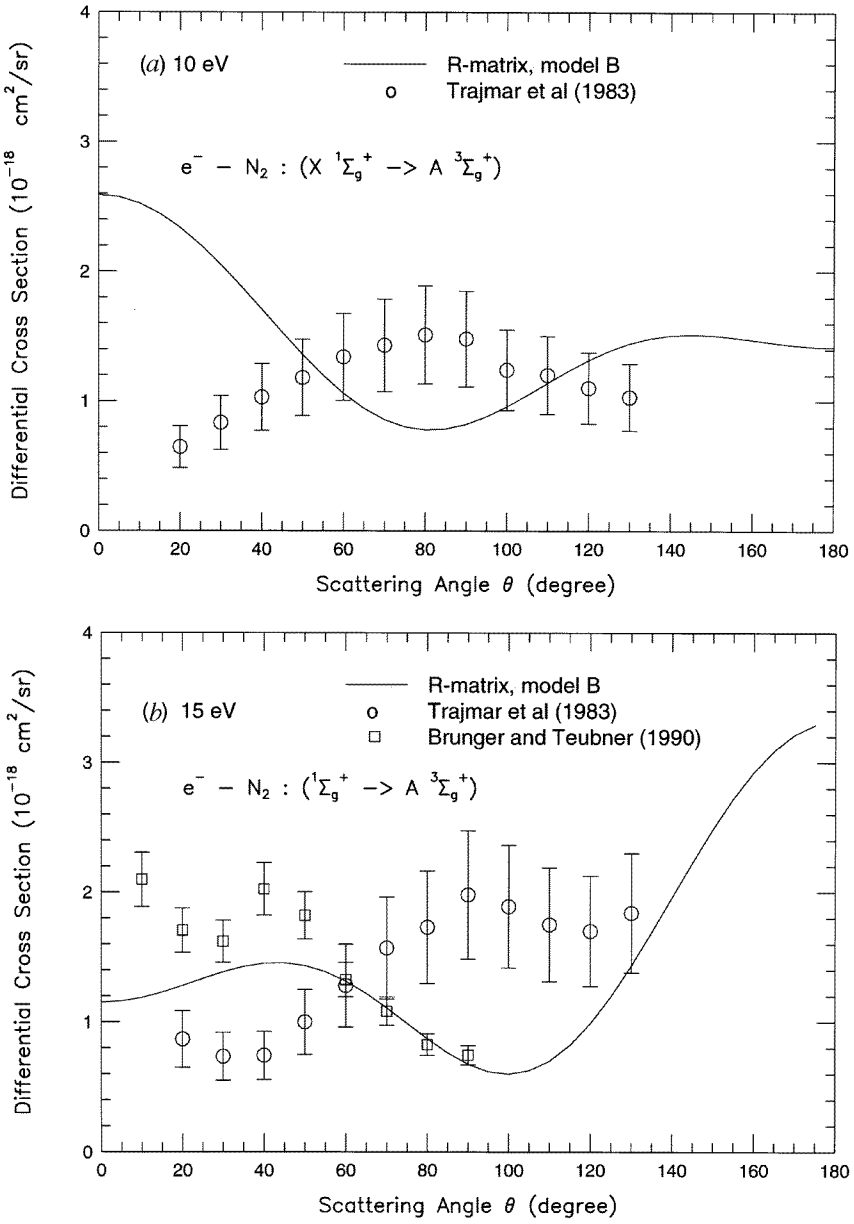

Figure 4. Differential cross sections at (*a*) 10 eV and (*b*) 15 eV impact energies for the transition $X\ ^1\Sigma_g^+ \rightarrow A\ ^3\Sigma_u^+$; the units are 10^{-18} cm^2 per steradian. The full curves are our calculated data using model B while the experimental data from Trajmar *et al* (1983), ○ , and from Brunger and Teubner (1990), □, are shown for comparison.

electron) targets. The application of such expansions to a molecule like nitrogen is at present well beyond the bounds of computational possibility. In particular, recent calculations using the Kohn variational principle (Rescigno 1994) suggest that electron molecule calculations may prove particularly poorly convergent with respect to the inclusion of target states.

After highlighting the differences between models A, B and C it may appear somewhat

surprising that the results we report here were only moderately sensitive to the choice of these models. However the differences between these models are entirely dependent on the (virtual) target orbitals outside the CAS which are retained in the calculation. After much experimentation we chose only to retain a single virtual orbital of each symmetry, many fewer than have been used in some calculations (e.g. Morgan 1991). Undoubtedly the shortness of this expansion tends to suppress some of the differences between the models.

We now turn to the comparison of $^2\Pi_g$ resonance positions given in table 5. Previous studies of this resonance (Morgan 1986, Gillan *et al* 1987, 1988 and references therein) have all been performed using single configuration (SCF) target wavefunctions. It is a general feature of moving from an SCF to a CI target that resonances move up in energy and broaden. This behaviour is a reflection of the better treatment of the *N* electron problem and is clearly displayed here. Recovery of the correct behaviour of the resonance with the improved target wavefunction requires either the inclusion of more targets in the close coupling expansion or some other means of recovering polarization effects which are present in the models based on SCF targets but difficult to include reliably for a CI target.

It is interesting to note the comparative stability of our calculations compared to the model employed in previous calculations. For example, Gillan *et al* (1988) found positions which varied by more than 1 eV and widths by a factor of two in calculations which differed by far fewer 2p–1h CSFs than the models employed here.

It would be desirable to conclude this section with a firm recommendation as to how to generate reliable wavefunctions for electron impact electronic excitation calculations. Unfortunately all three models employed here have positive and negative aspects; the appropriate model for a particular calculation is therefore likely to remain a matter of judgement.

6. Conclusions

This paper presents detailed results of an application of the *R*-matrix method to electronic excitation of the target in e^-–N_2 scattering; integrated cross sections have been computed and compared with experiment for optically forbidden transitions from the ground state. In this work we have refined and extended an existing model for the treatment of projectile–target correlation and quantified the various levels within our scheme for one test case. The results obtained compare favourably with existing experiments and our computations also yield a wealth of data on other scattering energies where no measured data are yet available. This will be reported in detail elsewhere (Gillan and McLaughlin 1996).

The major limitation of the present model is that the nuclei have been constrained to a single fixed geometry. Unfortunately, it is not straightforward to generalize this calculation to include nuclear motion. This is because the eight state approximation used here would not be valid as one approaches either the united atom or the dissociation limits. It is clear from the potential energy diagram for N_2 (see figure 1) that the $A'\ ^3\Sigma_g^+$, $C\ ^3\Pi_u$ and $G\ ^3\Delta_g$ states would have to be included in the model beyond $\sim 2.75\ a_0$.

We are, however, extending our *R*-matrix codes to handle a larger number of more accurate states (Tennyson 1996). This should lead not only to calculations which can treat the full range of internuclear separations reliably, but also to ones which can treat the many other electronic excitations in the system which have yet to be the subject of a high-level theoretical treatment. Extra target states are also required to give a reliable treatment of the $^2\Pi_g$ resonance within the present models.

The knowledge gained in studying this system is already playing a vital role in the *R*-matrix calculations on electron scattering by diatomic molecules of similar size. It

will also prove invaluable in the study of electron impact excitation of heavier and larger molecular systems.

Acknowledgments

The N_2 structure calculations were performed with the Alchemy II codes (McLean *et al* 1991) from the IBM MOTECC package. This was obtained under license from IBM. BMMcL thanks the Minnesota Supercomputer Institute for the award of a visiting fellowship during the course of this work and for computing resources on Cray architectures where some of these calculations were performed. CJG and JT would like to thank the Institute for Theoretical Atomic and Molecular Physics for the provision of visiting scientist funds. The Institute for Theoretical Atomic and Molecular Physics at the Harvard-Smithsonian Center for Astrophysics is supported by a grant from the National Science Foundation to Harvard University and the Smithsonian Astrophysical Observatory. This work was supported by the UK Engineering and Physical Sciences Research Council via Collaborative Computational Project Two (CCP2) and other grants.

References

Ajello J M and Shemansky 1985 *J. Geophys. Res.* **90** 9845
Baluja K L, Burke P G and Morgan L A 1982 *Comput. Phys. Commun.* **27** 299
Borst W L 1972 *Phys. Rev.* A **5** 648
Branchett S E, Tennyson J and Morgan L A 1990 *J. Phys. B: At. Mol. Opt. Phys.* **23** 4625–39
Bray I and Stelbovics A T 1995a *Adv. At. Mol. Opt. Phys.* **35** 209–54
——1995b *Comput. Phys. Commun.* **85** 1
Brunger M J and Teubner P J O 1990 *Phys. Rev.* A **41** 1413
Burke P G and Berrington K A 1993 *Atomic and Molecular Processes: an R-Matrix Approach* (Bristol: IOP)
Cartwright D C, Chujtian A, Trajmar S and Williams W 1977a *Phys. Rev.* A **16** 1013
Cartwright D C, Trajmar S, Chutjian A and Williams W 1977b *Phys. Rev.* A **16** 1041
Dalgarno A, Victor G A and Hartquist T W 1981 *Geophys. Res. Lett.* **8** 603
Dalgarno A and Victor G A 1982 *Geophys. Res. Lett.* **9** 866
Dalgarno A and Fox J L 1994 *Unimolecular and Bimolecular Reaction Dynamics* ed C Y Ng, T Baer and I Powis (New York: Wiley) pp 1–85
Ermler W C and McLean A D 1980 *J. Chem. Phys.* **73** 2297
Ermler W C, McLean A D and Mulliken R S 1981 *IBM Res. Rep.* **RJ3243** 1
Fox J L 1993 *Dissociative Recombination: Theory Experiment and Applications* ed B R Rowe, J B A Mitchell and A Canosa (New York: Plenum) p 219
Fox J L and Dalgarno A 1979 *Planet Space Sci.* **27** 491
Fox J L and Victor G A 1988 *Planet Space Sci.* **36** 329
Filippelli A R, Chung S and Lin C C 1984 *Phys. Rev.* A **29** 1709
Gillan C J and McLaughlin B M 1996 *At. Data and Nucl. Data Tables* to be submitted
Gillan C J, Nagy O, Burke P G, Morgan L A and Noble C J 1987 *J. Phys. B: At. Mol. Phys.* **20** 4585–603
Gillan C J, Noble C J and Burke P G 1988 *J. Phys. B: At. Mol. Opt. Phys.* **21** L53–9
——1990 *J. Phys. B: At. Mol. Opt. Phys.* **23** L407
Gillan C J, Tennyson J and Burke P G 1995 *Computational Methods for Electron Molecule Collisions* ed W M Huo and F Gianturco (New York: Plenum) pp 239–52
Huo W M 1990 *Nonequilibrium Processes in Partially Ionized Gases (NATO ASI Series)* ed M Capitelli and J N Bardsley (New York: Plenum) p 341
——W M 1995 *Computational Methods for Electron Molecule Collisions* ed W M Huo and F Gianturco (New York: Plenum) pp 327–53
Huo W M, Pritchard H, Watari K, Lima M A P and McLoy V 1987 *Abstr. 15th Int. Conf. Physics of Electronic and Atomic Collisions* ed J Geddes, H B Gilbody, A E Kingston, C J Latimer and H R J Walters (Belfast: Queen's University of Belfast) p 290
Higgins K, Noble C J and Burke P G 1994 *J. Phys. B: At. Mol. Opt. Phys.* **27** 3203

Higgins K, Gillan C J, Burke P G and Noble C J 1995 *J. Phys. B: At. Mol. Opt. Phys.* **28** 3391–402
Itkawa Y, Hayashi M, Ichimura A, Onda K, Sakimoto K, Takayanagi K, Nakamura M, Nishimura H and Takayanagi T 1986 *J. Phys. Chem. Ref. Data* **15** 985
Liu B and Yoshimine M 1980 *IBM Res.* **2849** 1
Liu W and Victor G A 1994 *Astrophys. J.* **435** 909
Malégat L 1990 *Comput. Phys. Commun.* **60** 391
Mason N J and Newell W R 1987 *J. Phys. B: At. Mol. Phys.* **20** 3913
Massey H S W and Mohr C B O 1932 *Proc. R. Soc.* A **136** 289
Morgan L A 1986 *J. Phys. B: At. Mol. Phys.* **19** L439–45
——1991 *J. Phys. B: At. Mol. Opt. Phys.* **24** 4649
Morgan L A and Tennyson J 1993 *J. Phys. B: At. Mol. Opt. Phys.* **26** 2429
McLaughlin B M and Gillan C J 1995 *Computational Methods for Electron Molecule Collisions* ed W M Huo and F Gianturco (New York: Plenum) pp 255–64
McLaughlin B M, Gillan C J, Burke P G and Dahler J S 1993 *Phys. Rev.* A **47** 1987
McLean A D, Yoshimine M, Lengsfield B H III, Bagus P S and Liu B 1991 *MOTECC Modern Techniques in Computational Chemistry* ed E Clementi (Leiden: ESCOM Science BV) p 23
Noble C J and Burke P G 1992 *Phys. Rev. Lett.* **68** 2011
Noble C J and Nesbet R K 1984 *Comput. Phys. Commun.* **33** 399
Orel A E, Rescigno T N and Lengsfield B H III 1991 *Phys. Rev.* A **44** 4330
Rescigno T N 1994 *Phys. Rev.* A **50** 1382–9
Rescigno T N, McCurdy C W, Orel A E and Lengsfield B H III 1995 *Computational Methods for Electron Molecule Collisions* ed W M Huo and F Gianturco (New York: Plenum) pp 1–37
Schematovich V I, Bisikalo D V and Gérard J C 1992 *Ann. Geophys.* **10** 792
Schneider F and Gianturco F A 1996 *J. Phys. B: At. Mol. Opt. Phys.* at press
Tennyson J 1988 *J. Phys. B: At. Mol. Opt. Phys.* **21** 805
——1996 *J. Phys. B: At. Mol. Opt. Phys.* at press
Trajmar S, Register D F and Chutjian A 1983 *Phys. Rep.* **7** 219
Zetner P W and Trajmar S 1987 *Proc. 15th Int. Conf. Physics of Electronic and Atomic Collisions* ed J Geddes, H B Gilbody, A E Kingston, C J Latimer and H R J Walters (Belfast: Queen's University of Belfast) Abstracts p 307
Zipf E C and Gorman M R 1980 *J. Chem. Phys.* **73** 813
Zipf E C and McLaughlin R W 1978 *Planet Space Sci.* **26** 449